PRECISE CALIBRATION OF HYDROPHONES IN A LABORATORY WATER TANK

Alexander E. Isaev, VNIIFTRI, RUSSIA

1 INTRODUCTION

The characteristic size of a measuring hydrophone can substantially exceed the dimensions of its active element. In this case it is difficult to achieve in a laboratory water tank the free field conditions at which the hydrophone to be calibrated is exposed to a practically plane acoustic wave. The interference between the incident wave emitted by the projector and the waves reflected from parts of hydrophone structure and its support distorts the measurement results. This paper describes a free field calibration procedure in which the measuring hydrophone is modelled by a point active element and a finite number of point reflectors [1].

2 REDUCED TRANSFER IMPEDANCE

Generally, the auxiliary transducers (both projectors *P* and transducers *T*) used in reciprocity calibration would have a special design providing minimal dimensions. However, measuring hydrophones usually have a housing and supports and their dimensions could be so large that it becomes impossible to satisfy “the minimum distance criteria” in a laboratory water tank. Consequently, the measurements are performed in an area where interference between the direct acoustic signal and that reflected from the body of the hydrophone and its support can cause distortion of the acoustic field. If the standard calibration procedure is used it will lead to large uncertainty of the results [2].

The influence of the measuring hydrophone on the acoustic field can be analysed using a simple model. Assume that the projector and the hydrophone are separated by a distance sufficient for their active elements to be represented by a point projector *P* with transmitting sensitivity $\dot{S}'_P$ and a point receiver *H* having sensitivity $\dot{M}'_H$. The reflecting properties of the body of the hydrophone and the support can be approximated by a point-like reflector *R* with a complex reflection coefficient $\dot{w}_R = w_R e^{-j\varphi_R}$. Elements *P*, *H* and *R* are located in XZ-plane as shown in Fig. 1. Receiver *H* is placed at the origin of co-ordinates, while projector *P* lies on the X-axis at the point (x_1, 0), reflector *R* being localised at (0, z_R).
The acoustic pressure acting on the receiver *H* is the result of the interference between two coherent spherical waves, i.e. the incident wave with the complex amplitude:

$$\dot{p}_{PH} = \dot{S}'_P \dot{I}_{PH} \frac{r_0}{r_{PH}} e^{-jk\left(r_{PH} - r_0\right)}$$

and the reflected wave with the complex amplitude:

$$\dot{p}_{RH} = w_R \dot{S}'_P \dot{I}_{PH} \frac{r_0}{r_{PR}+r_{RH}} e^{-j\left(k\left(r_{PR}+r_{RH}-r_0\right)+\varphi_R\right)} ,$$

where:

$\dot{I}_{PH}$ - is electrical current through projector P,

r_0 – is the reference distance, usually equal to 1m,

$k = \dfrac{2\pi f}{c}$ – is the wavenumber,

f – is the frequency of the acoustic signal,

c – is the sound speed in water.

The equation for the complex voltage $\dot{U}_{PH}$ at the output of the hydrophone can be written as:

$$\dot{U}_{PH} = \dot{M}'_H \dot{S}'_P \dot{I}_{PH} \frac{r_0}{r_{PH}} e^{-jk\left(r_{PH}-r_0\right)}\left(1+w_R y_R\left(r_{PH}\right)e^{-j\left(k\vartheta_R+\varphi_R\right)}\right). \quad (1)$$

where:

$$\upsilon_R = r_{PR}+r_{RH}-r_{PH} ,$$

$$0 < y_R\left(r_{PH}\right) = \frac{r_{PH}}{r_{PR}+r_{RH}} \leq 1 .$$

Our further derivations are based on the concept of electrical transfer impedance reduced according to the law of the acoustic wave propagation. For source P and hydrophone H separated by a distance r_{PH} the electrical transfer impedance reduced to the spherical wave propagation (further called *reduced transfer impedance, RTI*) can be represented in the form:

$$\dot{Z}_{PH}(r) = \frac{\dot{U}_{PH}}{\dot{I}_{PH}} \frac{r_{PH}}{r_0} e^{jk\left(r_{PH}-r_0\right)} . \quad (2)$$

The reduced transfer impedance of a point-like projector P and a point-like receiver H in the undisturbed acoustic field of the spherical wave is independent of the distance between P and H and is equal to $\dot{M}'_H \dot{S}'_P$. This impedance is denoted $\dot{Z}_{PH0}$.

In the field of a spherical wave disturbed by the wave coming from the reflector the reduced transfer impedance will depend on the distance between the source and the receiver. Substituting the expression for the hydrophone output voltage, eq. (1), into eq.(2) for w_R << 1, the following approximate formula for the magnitude of the RTI can be written:

$$Z_{PH}(r) = Z_{PH0}\sqrt{\left(1+2w_R y_R\left(r_{PH}\right)\cos\left(k\upsilon_R+\varphi_R\right)\right)} , \quad (3)$$

where

$$Z_{PH0} = M'_H S'_P .$$

Fig. 2 shows experimental values (in relative units) of the RTI of the projector and the hydrophone obtained at 30 kHz, 40 kHz and 60 kHz. Two piezoelectric spheres 7 mm in diameter mounted on a thin electrical cable were used both as the projector and the hydrophone. A reflector in the form of a hollow sphere 30 mm in diameter was mounted on the hydrophone cable 250 mm above the active element. During the measurements the distance between the transducers varied in the range 400 mm to 1540 mm.

From Figs. 1 and 2 it is seen that the increase in the distance between the transducers results in the decrease of the ray path difference $\Delta r = r_{PR} - r_{PH}$ between the direct acoustic ray from projector *P* to hydrophone *H* and the ray from projector to reflector. Hence, the phase difference between the direct and the reflected acoustic waves that sum up at the hydrophone location, also changes. As the projector is moving from its original position to infinity the reduced transfer impedance at a given frequency *f* makes $\frac{\Delta r_1}{\lambda}$ oscillations with decaying spatial period (here λ is the acoustic wavelength). For $r_{PH} >> \frac{r_{RH}^2}{\lambda}$ the magnitude on the reduced transfer impedance approaches a constant value:

$$Z_{PH\infty} = Z_{PH0}\sqrt{(1+2w_R\cos(kr_{RH}+\varphi_R))}. \qquad (4)$$

For the receiving sensitivity M_H of the hydrophone considered as a system of a point-like active element and a point-like reflector the following expression can be written:

$$M_H = M'_H\sqrt{(1+2w_R\cos(kr_{RH}+\varphi_R))}.$$

A similar relation is valid for the transmitting sensitivity S_P of the projector in the case when the hydrophone is point-like and the reflector is localised on the projector:

$$S_P = S'_P\sqrt{(1+2w_R\cos(kr_{RH}+\varphi_R))}.$$

When the electrical transfer impedance determined for arbitrary distances between the transducers is used in the calculation of the hydrophone sensitivity the results can contain significant error. As can be seen from Fig. 2 the difference of the RTI value from $Z_{PH\infty}$ may reach twice the amplitude of the envelope, which accounts about 7% at 30 kHz and 6% at 40 kHz.

Let us formulate the problem of determining $Z_{PH\infty}$ using the values of the reduced transfer impedance $Z_{PH}(r)$.

3 TECHNIQUE TO FIND THE REFLECTOR CO-ORDINATES

The following technique can be applied to find the reflector co-ordinates. Suppose, for a set of distances r_{PHi} (*i*=1,…,N) the squares of the RTI modules $Z^2_{PH}(r)_i$ are known. A virtual point-like reflector *V* with unity reflection coefficient is placed in some point of the plane with co-ordinates (x_V, z_V), see Fig. 1. For this virtual reflector *V* on an aperture $D \in (r_{PHi}$, *i*=1,…,N) a functional $Q(V, D)$ can be defined as:

$$Q(V,D) = \frac{1}{\|\hbar(V,D)\|}\sqrt{\left(Q'(V,D)\right)^2 + \left(Q''(V,D)\right)^2}\,, \qquad (5)$$

where:

$$Q'(V,D) = \sum_{i=1}^{N} \aleph_i \; y_V\left(r_{PH\,i}\right)\cos\left(k\,\upsilon_{V\,i}\right),$$

$$Q''(V,D) = \sum_{i=1}^{N} \aleph_i \; y_V\left(r_{PH\,i}\right)\sin\left(k\,\upsilon_{V\,i}\right),$$

$$\aleph_i = \frac{Z_{PH}^2\,(r)_i}{Z_{PH\,0}^2} - 1\,,$$

$$\upsilon_{V\,i} = r_{PV\,i} - r_{PH\,i} + r_{VH}\,,$$

$\hbar(V,D)$ – is scaling function.

It is easy to show that the functional $Q(V,D)$ has global maximum in the point with co-ordinates (x_V =x_R, z_V=z_R). Consequently, scanning a part of the plane $x_V \in (x_R - a, x_R + a)$, $z_V \in (z_R - b, z_R + b)$ in a presumable area of reflector *R* location and plotting in intensity levels the values of $Q(V,D)$ for each location of reflector *V* one can obtain an acoustic image of reflector *R* as a bright spot on the intersection of two rays in the point with co-ordinates (x_R, z_R).

Figs. 3a-5a show acoustic images of the reflector at 30 kHz, 40 kHz and 60 kHz obtained using the RTIs represented in Fig. 2. In the calculation of the functional in eq.(5) the following approximation was used:

$$Z_{PH\,0} \approx \frac{1}{N}\sum_{i=1}^{N} Z_{PH}\,(r)_i \quad .$$

The virtual reflector scanned the area in the range from –400 mm to +400 mm along the X-axis and from 0 mm to 700 mm along the Z-axis, the centre of the source active element being at the origin of co-ordinates. Figs. 3b-5b show numerical values of the functional on the Z-axis. In all the three images the functional $Q(V,D)$ reaches its maximum at the same area of the plane close to the point (0,250) which is in good agreement with experiment. It also confirms the stability of the method.

4 MODEL OF REFLECTING SURFACE OF A HYDROPHONE

The proposed method was used to restore the reflecting surface of a hydrophone being calibrated. Circles in Fig. 6 represent experimental magnitudes of the RTI in relative units at 40 kHz, 60 kHz and 120 kHz as a function of distance for a B&K type 8104 hydrophone. The distance between the hydrophone and the projector was varied from 480 mm to 800 mm. During the measurements the hydrophone was installed vertically in a water tank at the depth of 3 m. The hydrophone was mounted by its cable to two thin titanium strings using a clip made of a plastic having acoustic impedance *ρc* close to that of water. The maximum dimension of the clip did not exceed 50 mm. The clip was fixed at 550-570 mm from the geometric centre of the hydrophone sensitive element. Piezoelectric spheres 20 mm (at the frequency of 40 kHz) and 7 mm in diameter (at 60 kHz and

120 kHz) were used as projectors. Radio-pulse mode measurements provided time selection of the signals reflected from the surfaces of the water tank.
The length of the pulse did not exceed 50 periods of the carrier frequency. The position of the geometric centre of the B&K type 8104 active element was taken as the origin of co-ordinates.
Experimental magnitudes of the RTI were used to obtain the acoustic images of the hydrophone reflecting surface. The virtual point-like reflector scanned an area within ±400 mm along the X-axis and from 0 mm to 700 mm along the Z-axis relative to the centre of the B&K type 8104 sensitive element. The resulting acoustic images are reproduced in Figs. 7a-9a. Numerical values of $Q(V,D)$ on an interval of the Z-axis are represented in Figs. 7b-9b (along this axis the body of the hydrophone, its cable and the clip were arranged). From Figs 7a and 7b it is clear that at the frequency of 40 kHz both the hydrophone body and its cable can be regarded acoustically transparent. A bright spot corresponding to the maximum of $Q(V,D)$ at the point (0,560) is the image of the clip. At 60 kHz the functional still has its maximum at (0,560) but the body of the hydrophone and the cable cease to be transparent and reveal themselves as an additional reflector localised at 230 mm from the sensitive element, see Figs 8a and 8b. At the frequency of 120 kHz (see Figs. 9a and 9b) the influence of the hydrophone body and the cable can be regarded as that of the reflector localised 170 mm from the sensitive element. No influence of the clip is apparent at 120 kHz due to time selection of the direct signal and the signal reflected from the clip.
It is convenient to approximate the resulting images using a simple model constructed from a set of point-like reflectors. If we place these reflectors at the points corresponding to the maximumes of $Q(V,D)$ on the Z-axis for each frequency we will get a simple model of the hydrophone, consisting of a point-like active element with sensitivity M'_H and a system of M point reflectors R_m (m = 1,…,M) with known co-ordinates and reflecting coefficients $\dot{w}_m$ to be determined.

5 ESTIMATION OF REDUCED TRANSFER IMPEDANCE PARAMETERS

. For w_m << 1 (m = 1,…,M) the square of the RTI magnitudes can be represented by the following function of 2M+1 unknowns $Z_0, w'_1, w''_1, \dots, w'_M, w''_M$:

$$Z^2(r_{PH}) = Z_0^2\left(1 + 2\sum_{m=1}^{M} y_m(r_{PH})\left(w'_m \cos\left(k\,\upsilon_m(r_{PH})\right) - w''_m \sin\left(k\,\upsilon_m(r_{PH})\right)\right)\right),$$

where :

$$\upsilon_m = r_{PRm} + r_{RmH} - r_{PH},$$

$$y_m(r_{PH}) = \frac{r_{PH}}{r_{PRm} + r_{RmH}},$$

$$w'_m = \mathrm{Re}(\dot{w}_m), \qquad w''_m = \mathrm{Im}(\dot{w}_m), \qquad m = 1,\dots,M.$$

The problem of determination of the unknowns in $Z^2(r_{PH})$ can be reduced to the well-known problem of optimal linear filtration for the equation of measurements having the form:

$$\Re_0 + \sum_{m=1}^{M} \Re'_m y_m(r_{PH\,i})\cos(k\,\upsilon_m(r_{PH\,i})) - \sum_{m=1}^{M} \Re''_m y_m(r_{PH\,i})\sin(k\,\upsilon_m(r_{PH\,i})) = \Im_i + \varepsilon_i,$$

where ε_i – is a random error, and the components of the unknown parameter vector have the form:

$$\Re_0 = Z_0^2,$$

$$\Re'_m = 2w'_m Z_0^2,$$

$$\Re''_m = 2w''_m Z_0^2.$$

Further we consider in details the case of estimating the RTI parameters taking into account uncertainty δ in the distances $r_{PH\,i}$ between the centres of transducer active elements. The transducers are assumed to be placed at the distances $d_{PH\,i}$ from each other. These distances can be chosen arbitrarily but need to be uniquely determined (as, for example, the distance between the suspension brackets of the hydrophone and the projector). Taking into consideration that $\delta = d_{PH\,i} - r_{PH\,i}$ and assuming $\delta << d_{PH\,i}$, we will come to the following expression for $Z^2(d_{PH})$:

$$Z_{PH}^2(d) = Z_{PH}^2(r) + 2\frac{\delta}{d_{PH} - \delta} Z_{PH}^2(r).$$

Then, the equation of measurements can be rewritten in a form that is more suitable for solution by iteration technique:

$$\Re_0 + \sum_{m=1}^{M} \Re'_m y_m(d_{PH\,i} - \delta)\cos(k\,\upsilon_m(d_{PH\,i} - \delta)) - \sum_{m=1}^{M} \Re''_m y_m(d_{PH\,i} - \delta)\sin(k\,\upsilon_m(d_{PH\,i} - \delta))$$

$$+ \tilde{\delta}\frac{2\Im_i}{d_{PH\,i}} = \Im_i + \eta_i \quad , \qquad (6)$$

where:

$$\Im_i = Z_{PH}^2(d)_i,$$

$$\eta_i = \frac{(r_i - \delta)}{r_i}\varepsilon_i.$$

At the first iteration the estimations for $\Re_0, \Re'_1, \Re''_1 \ldots, \Re'_M, \Re''_M$ and $\tilde{\delta}$ are calculated with $\delta = 0$. At further iterations the solutions of eq. (6) are found by replacing δ with $\tilde{\delta}$, obtained at a previous step. As a condition for stopping the iterations convergence of $\tilde{\delta}$ to a constant value can be used.

After the iteration procedure is finished the values of Z_0 and Z_∞ are calculated using the formulae:

$$Z_{PH0} = \sqrt{\Re_0},$$

$$Z_{PH\infty} = \sqrt{\Re_0 + \sum_{m=1}^{M} \left(\Re'_m \cos(k\, r_{RmH}) - \Re''_m \sin(k\, r_{RmH}) \right)} .$$

The proposed method enables the calculation the values of the transducer active element RTI Z_{PH0} as well as the far-field RTIs $Z_{PH\infty}$. The calculation of the RTI as a function of the distance between the transducers, $Z_{PH}(r)$, can also be performed. Other RTIs, Z_{PT0}, $Z_{PT\infty}$, Z_{TH0}, $Z_{TH\infty}$ are determined in a similar way. Solid lines in Figs. 2 and 6 show the results of the RTI approximation using the model of the hydrophone reflecting surface as a system of point-like reflectors. The resulting approximations are in good agreement with experimental data.

6 SENSITIVITY COMPUTATION

After the values of Z_{PH0}, $Z_{PH\infty}$, Z_{PT0}, $Z_{PT\infty}$, Z_{TH0}, $Z_{TH\infty}$ have been determined the hydrophone active element receiving sensitivity, M'_H is found from the formula:

$$M'_H = \left(\frac{2\, r_0}{pf} \frac{Z_{PH0} Z_{TH0}}{Z_{PT0}} \right)^{1/2} \tag{7}$$

The expression for the calculation of the hydrophone sensitivity M_H takes the form:

$$M_H = \left(\frac{2\, r_0}{pf} \frac{Z_{PH\infty} Z_{TH\infty}}{Z_{PT\infty}} \right)^{1/2} .$$

The performed investigation demonstrated that the proposed procedure significantly reduced the uncertainty caused by the distortion of the acoustic field.

Figs. 10a and 11a represent free-field calibration results for hydrophones H 52-50 and B&K 8104. The calibration was performed in a laboratory water tank by both the traditional technique for the calculation of the sensitivity [3] and the procedure described above. Curves 1 and 2 were obtained from two different standard facilities, implementing the standard reciprocity method. In the first case the measurements were made with a fixed distance between the transducers, while in the other the electrical transfer impedances were derived as an average result

of the two measurements made at different distances. Curves 3.1, 3.2 and 3.3 represent M'_H values calculated from eq. (7) in three frequency ranges. In each range different types of auxiliary transducers were used, providing the overlap of the frequency ranges (see the overlapping intervals of curves 3.1, 3.2 and 3.3). At these common frequencies the spread of calibration results acquired with various auxiliary transducers does not exceed 0.07 dB for hydrophone H 52-50 and 0.16 dB for B&K type 8104 (in these intervals curves 3.1, 3.2 and 3.3 in Figs. 10a and 11a practically coincide). The frequency responses of the both hydrophones are fairly smooth and change steadily, as opposed to the results of the traditional calibration procedure. There are no jump fluctuations at adjacent frequencies, which proves the accuracy of the proposed procedure. The calibration results from the traditional procedure in dB re. M'_H are reproduced in Figs. 10b and 11b, curves 1 and 2. The values of hydrophone sensitivity calculated by convential equation for the two standard facilities are markedly different from those of M'_H. This difference reaches 0.6 dB for hydrophone H 52-50 and 1.2 dB for B&K type 8104.
The behaviour of curves 1 and 2 in Figs. 10b and 11b is highly irregular and reflects the influence of the measurement uncertainty due to the distortion of the acoustic field in the water tank. This conclusion is most evident for hydrophone H 52-50 at low frequencies, where its frequency response has a flat region (see Fig. 10a).

7 REFERENCES

1. Russian Federation patent pending № 2002110963 class H04R29/00 “A technique for free-field reciprocity calibration of electroacoustic transducers”, priority from 24.04.2002.
2. K. Rasmussen, “Acoustic center of Condenser Microphones”, The Acoustics Laboratory, Technical University of Denmark. Report no.5, 1973
3. IEC Standard 565, *Calibration of hydrophones*, Geneva, International Electrotechnical Commission, 1977.

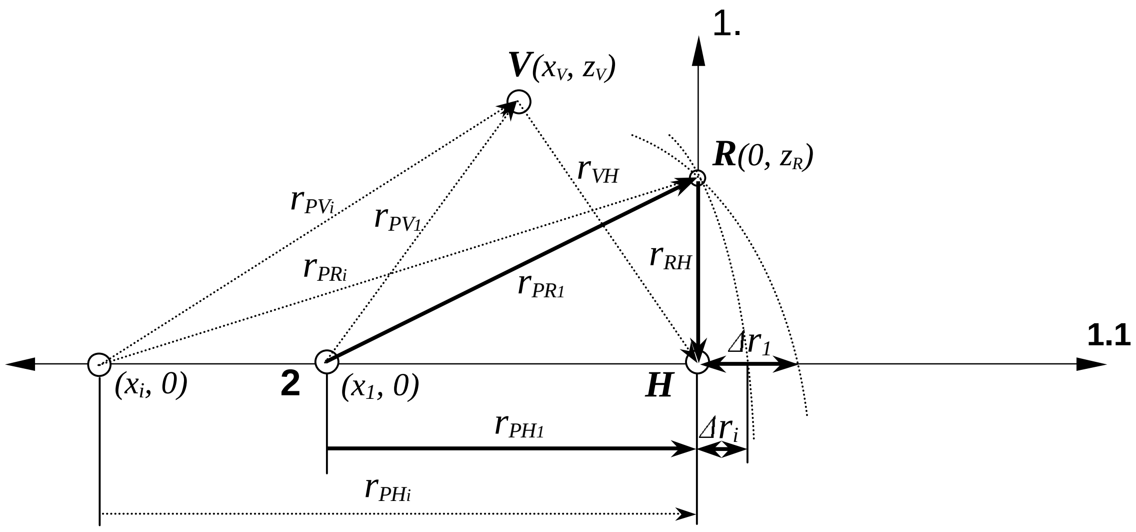
1.
V(xV, zV)
R(0, zR)
rVH
rPVi
rPV1
rPRi
rRH
rPR1
Δr1
1.1
(xi, 0)
2
(x1, 0)
H
rPH1
Δri
rPHi

Fig. 1

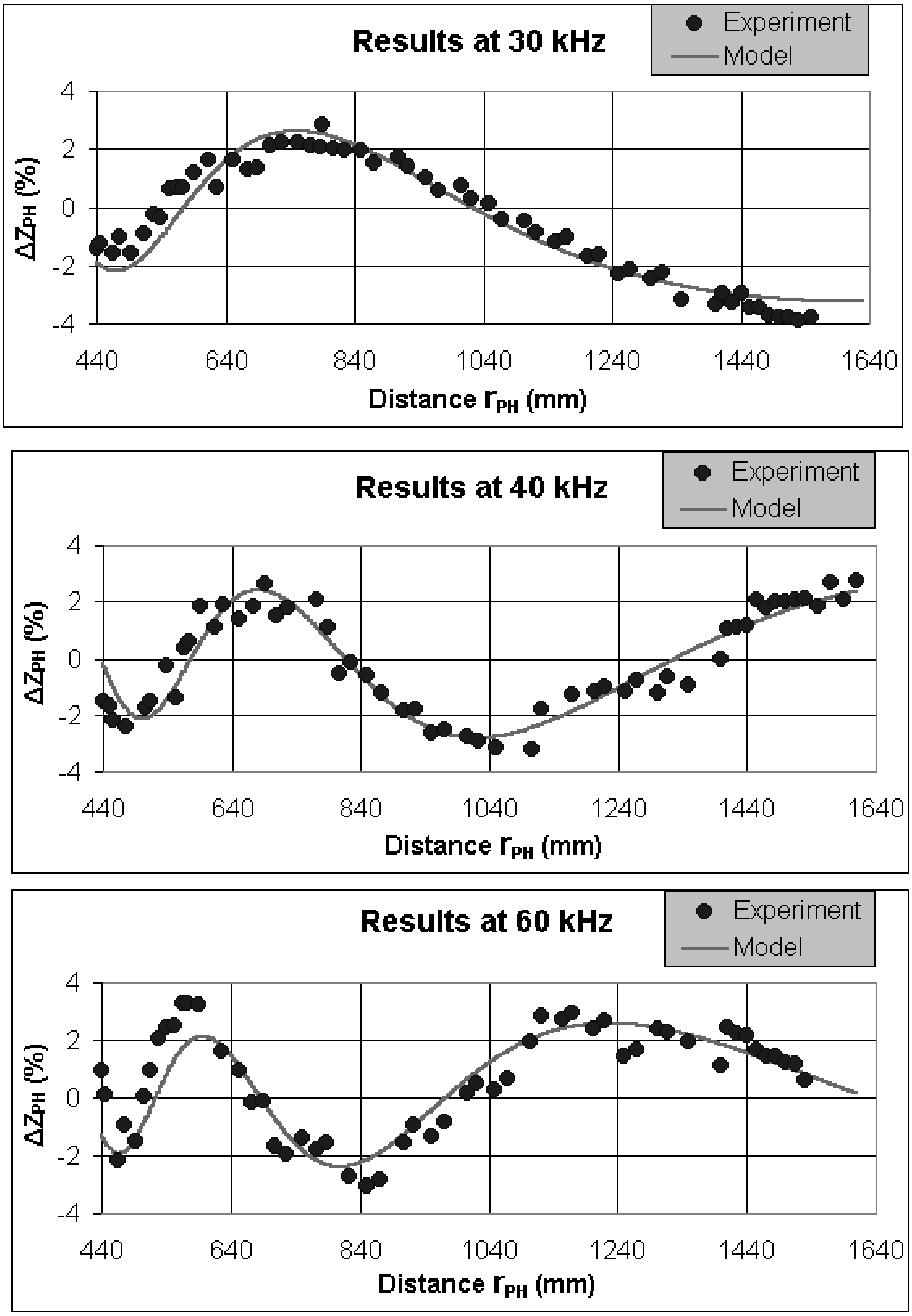
Results at 30 kHz
Experiment
Model
ΔZ_PH (%)
Distance r_PH (mm)
Results at 40 kHz
Experiment
Model
ΔZ_PH (%)
Distance r_PH (mm)
Results at 60 kHz
Experiment
Model
ΔZ_PH (%)
Distance r_PH (mm)

FIG. 2

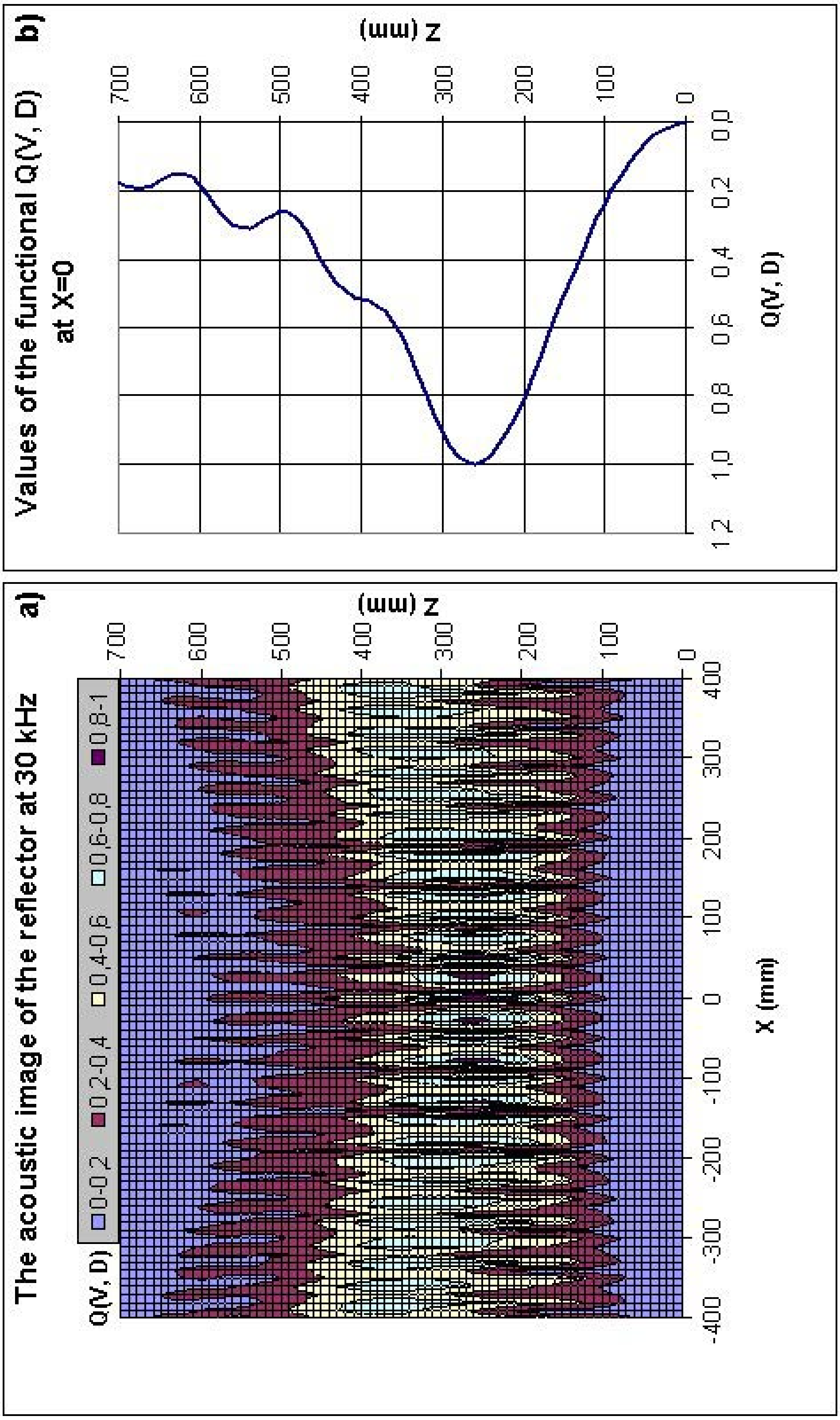
The acoustic image of the reflector at 30 kHz
a)
Q(V, D)
0-0,2
0,2-0,4
0,4-0,6
0,6-0,8
0,8-1
Z (mm)
X (mm)
Values of the functional Q(V, D) at X=0
b)
Z (mm)
Q(V, D)

Fig. 3

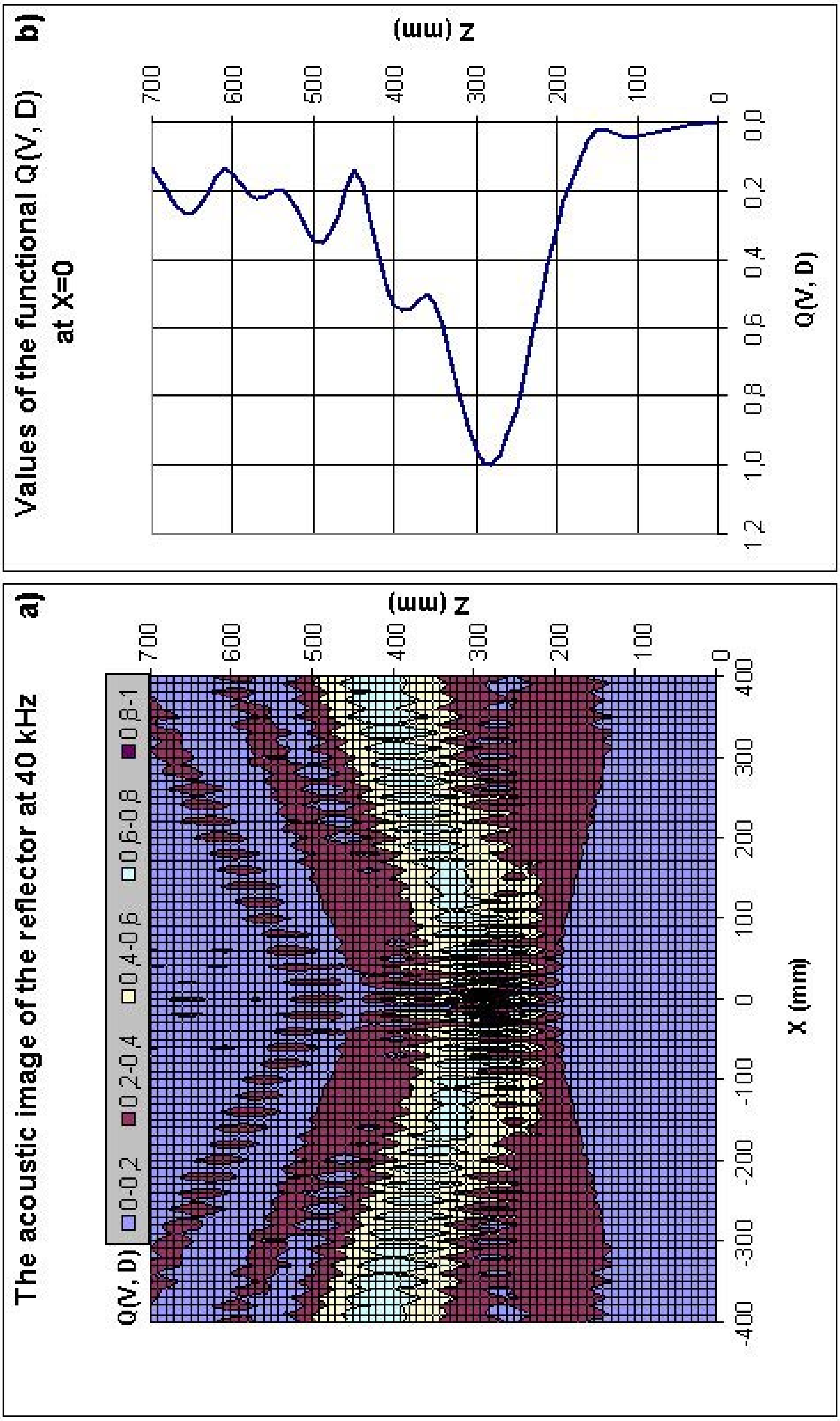
The acoustic image of the reflector at 40 kHz
a)
Q(V, D)
0-0.2
0.2-0.4
0.4-0.6
0.6-0.8
0.8-1
Z (mm)
X (mm)
Values of the functional Q(V, D) at X=0
b)
Z (mm)
Q(V, D)

Fig. 4

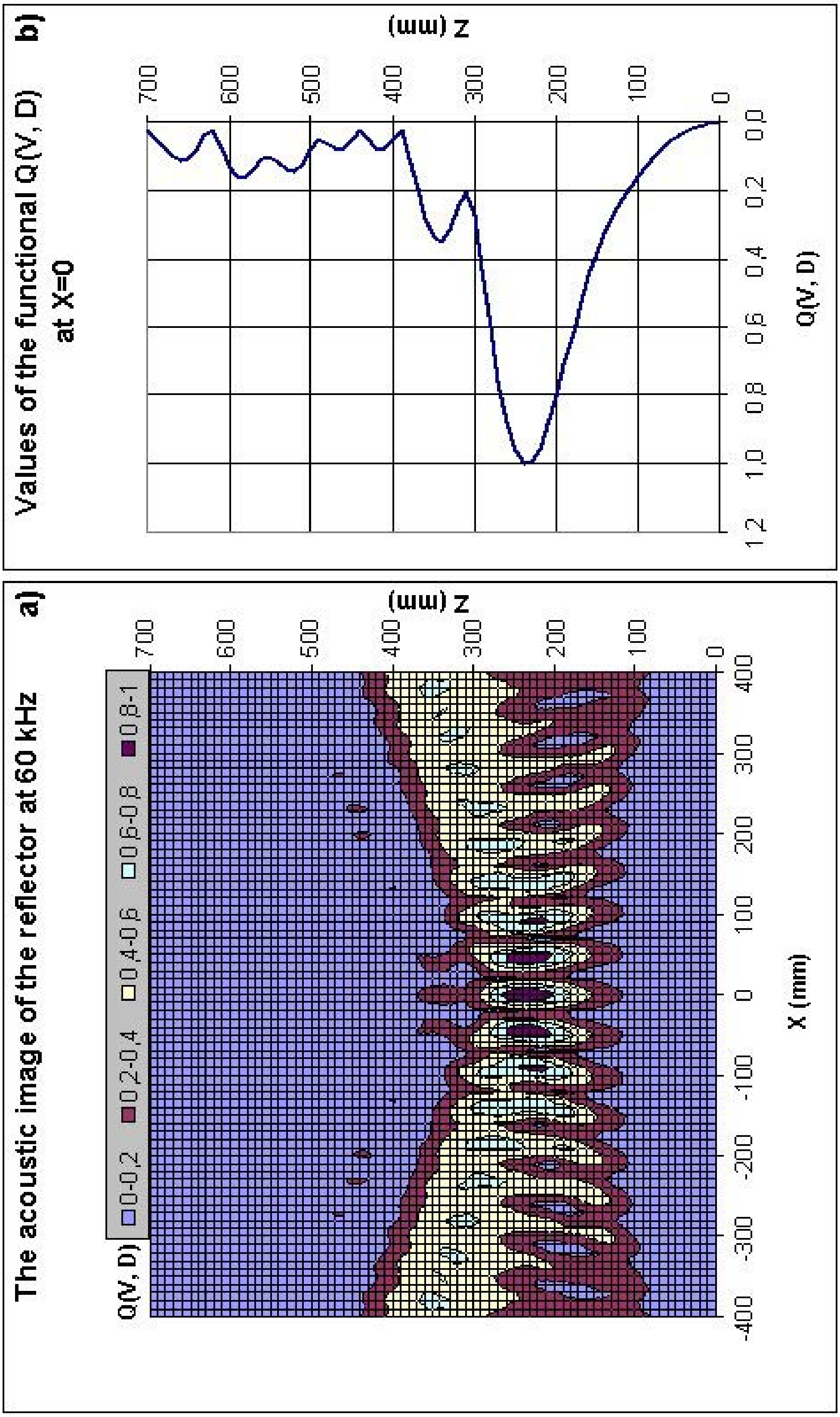
a)
The acoustic image of the reflector at 60 kHz
Q(V, D)
0-0,2
0,2-0,4
0,4-0,6
0,6-0,8
0,8-1
Z (mm)
700
600
500
400
300
200
100
0
X (mm)
-400
-300
-200
-100
0
100
200
300
400
b)
Values of the functional Q(V, D) at X=0
Z (mm)
700
600
500
400
300
200
100
0
Q(V, D)
0,0
0,2
0,4
0,6
0,8
1,0
1,2

Fig. 5

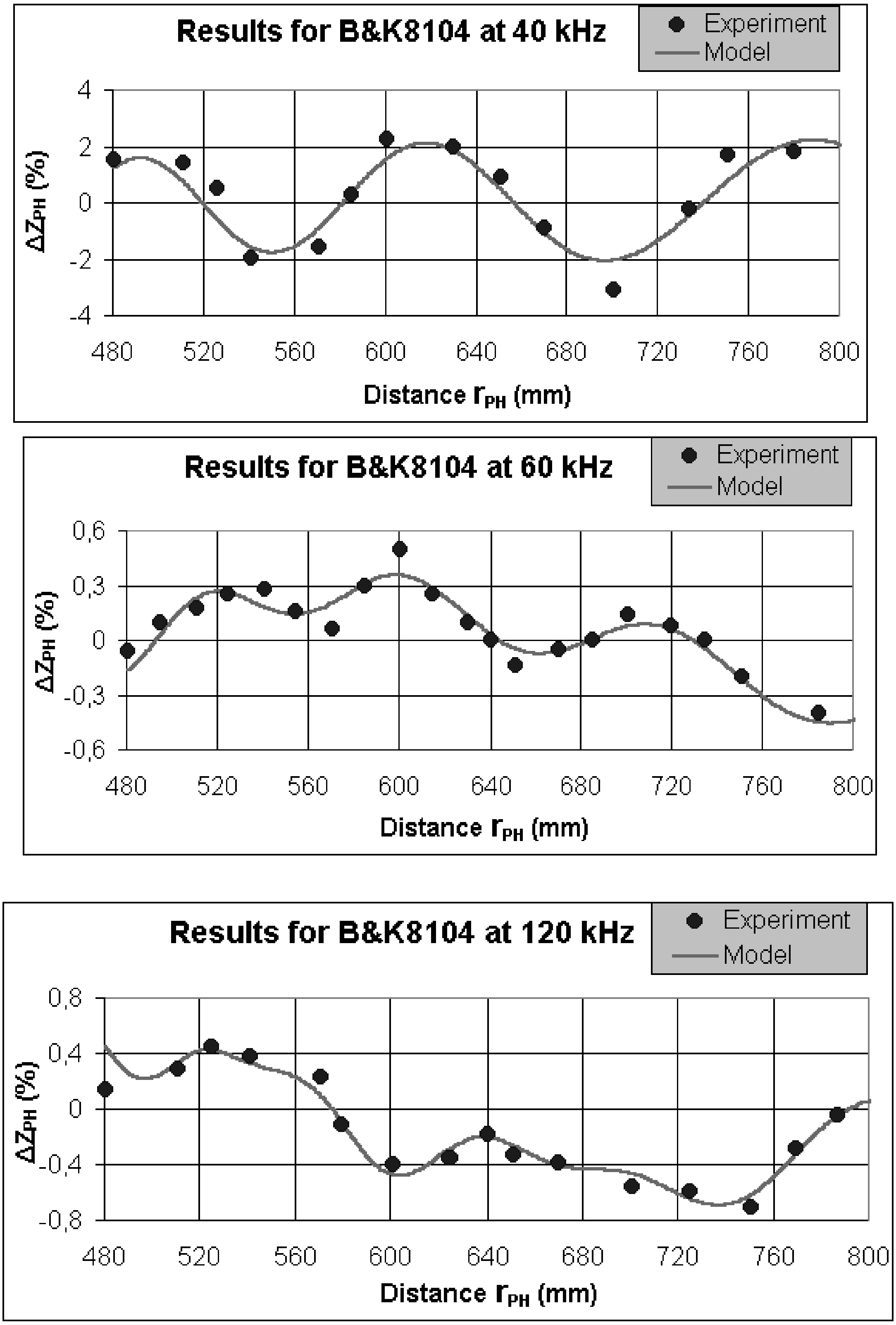
Results for B&K8104 at 40 kHz
Experiment
Model
4
2
0
-2
-4
ΔZ$_{PH}$ (%)
480
520
560
600
640
680
720
760
800
Distance r$_{PH}$ (mm)
Results for B&K8104 at 60 kHz
Experiment
Model
0,6
0,3
0
-0,3
-0,6
ΔZ$_{PH}$ (%)
480
520
560
600
640
680
720
760
800
Distance r$_{PH}$ (mm)
Results for B&K8104 at 120 kHz
Experiment
Model
0,8
0,4
0
-0,4
-0,8
ΔZ$_{PH}$ (%)
480
520
560
600
640
680
720
760
800
Distance r$_{PH}$ (mm)

FIG. 6

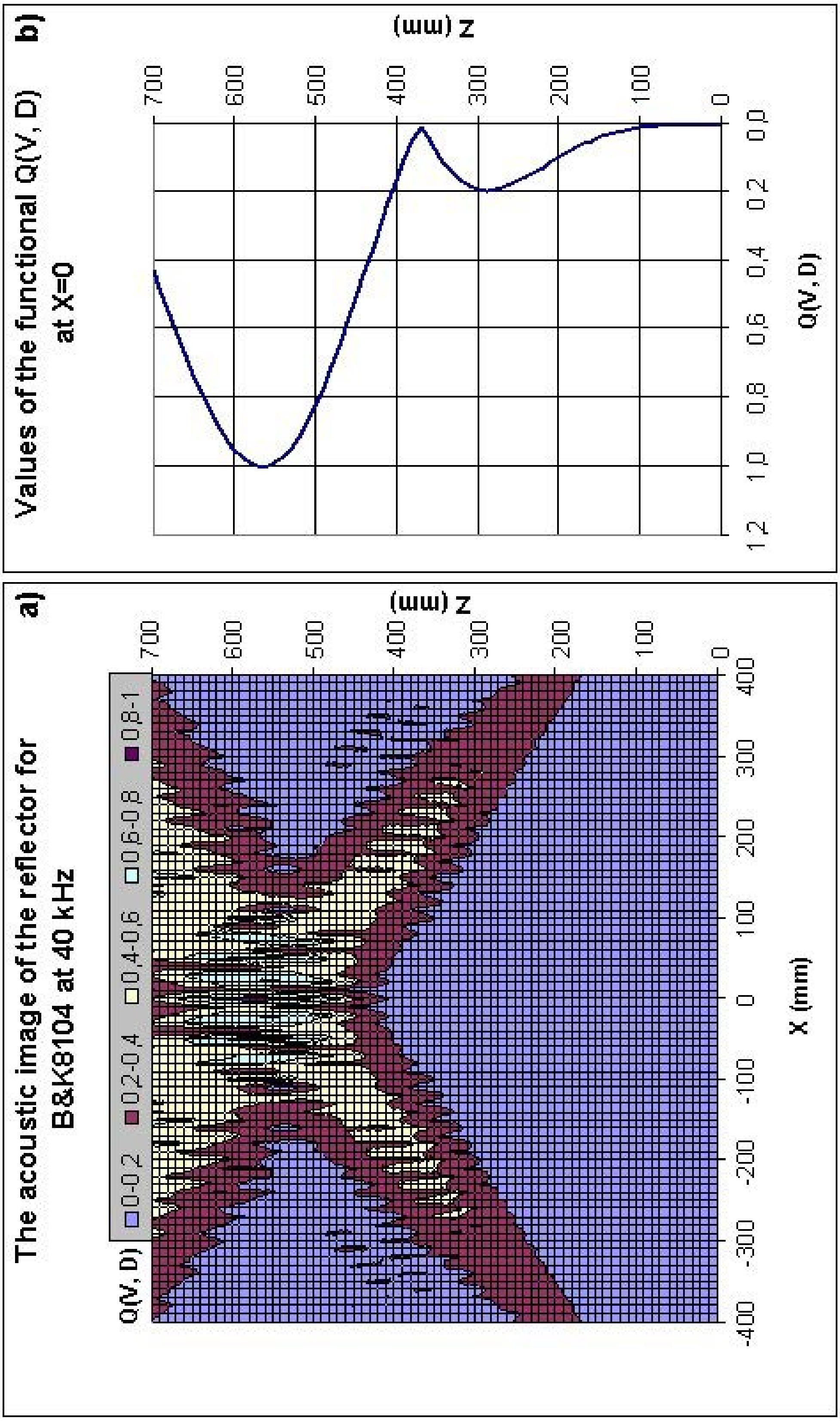
The acoustic image of the reflector for B&K8104 at 40 kHz
a)
Q(V, D)
0-0,2
0,2-0,4
0,4-0,6
0,6-0,8
0,8-1
Z (mm)
X (mm)
Values of the functional Q(V, D) at X=0
b)
Z (mm)
Q(V, D)

Fig. 7

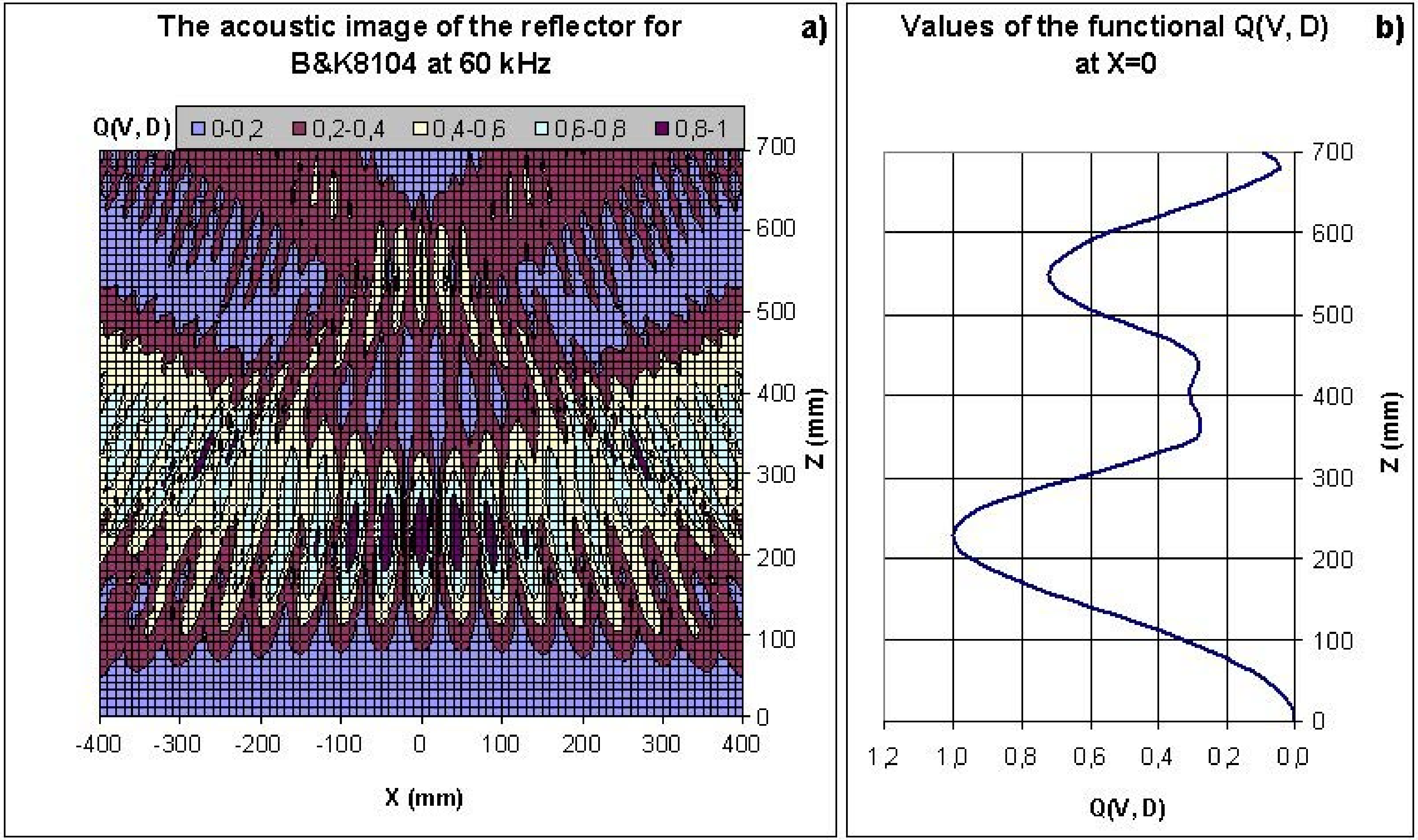
The acoustic image of the reflector for
B&K8104 at 60 kHz
a)
Q(V, D)
0-0,2
0,2-0,4
0,4-0,6
0,6-0,8
0,8-1
X (mm)
Z (mm)
Values of the functional Q(V, D)
at X=0
b)
Q(V, D)
Z (mm)

Fig. 8

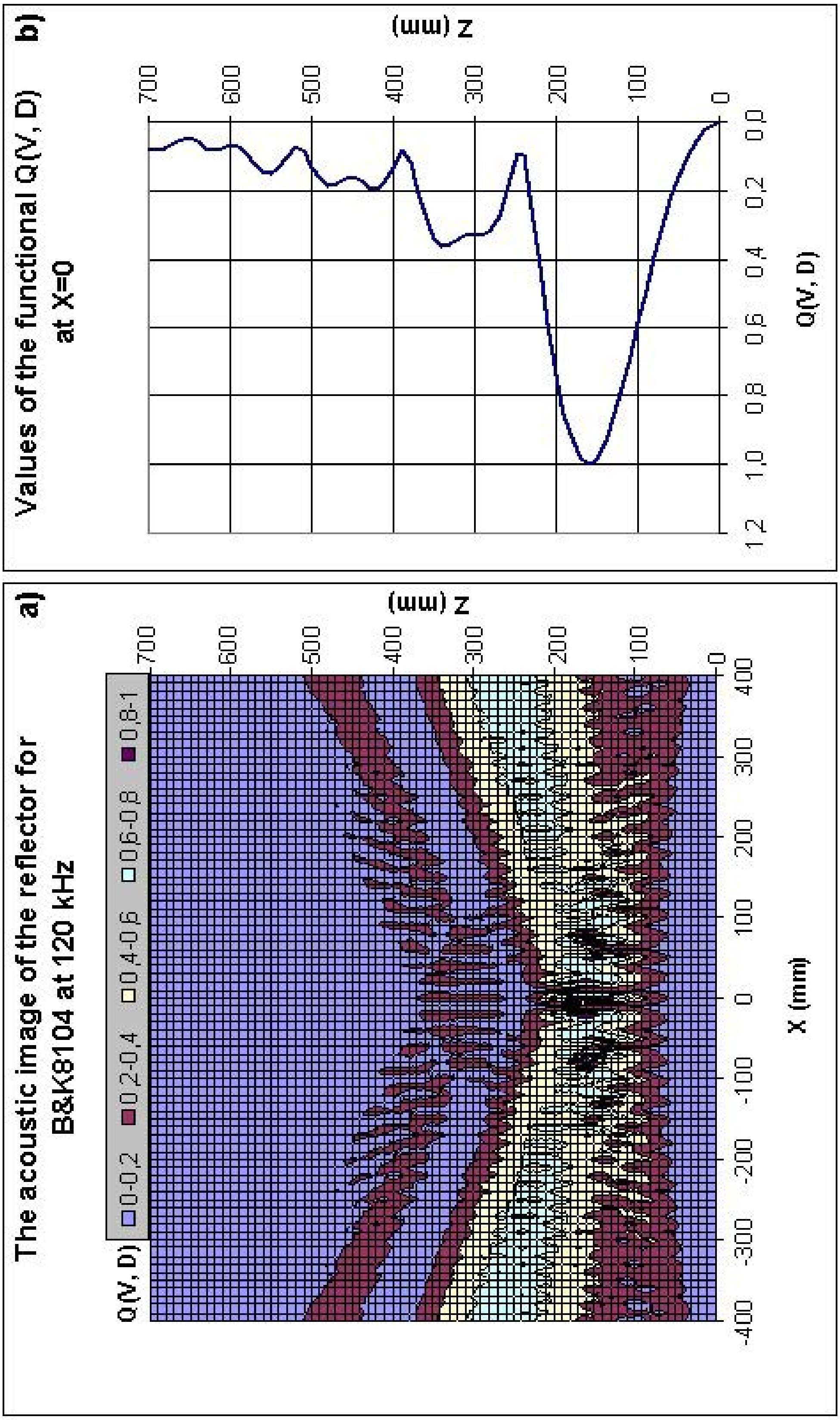
a)
The acoustic image of the reflector for
B&K8104 at 120 kHz
Q(V, D)
0-0,2
0,2-0,4
0,4-0,6
0,6-0,8
0,8-1
Z (mm)
700
600
500
400
300
200
100
0
-400
-300
-200
-100
0
100
200
300
400
X (mm)
b)
Values of the functional Q(V, D)
at X=0
Z (mm)
700
600
500
400
300
200
100
0
0,0
0,2
0,4
0,6
0,8
1,0
1,2
Q(V, D)

Fig. 9

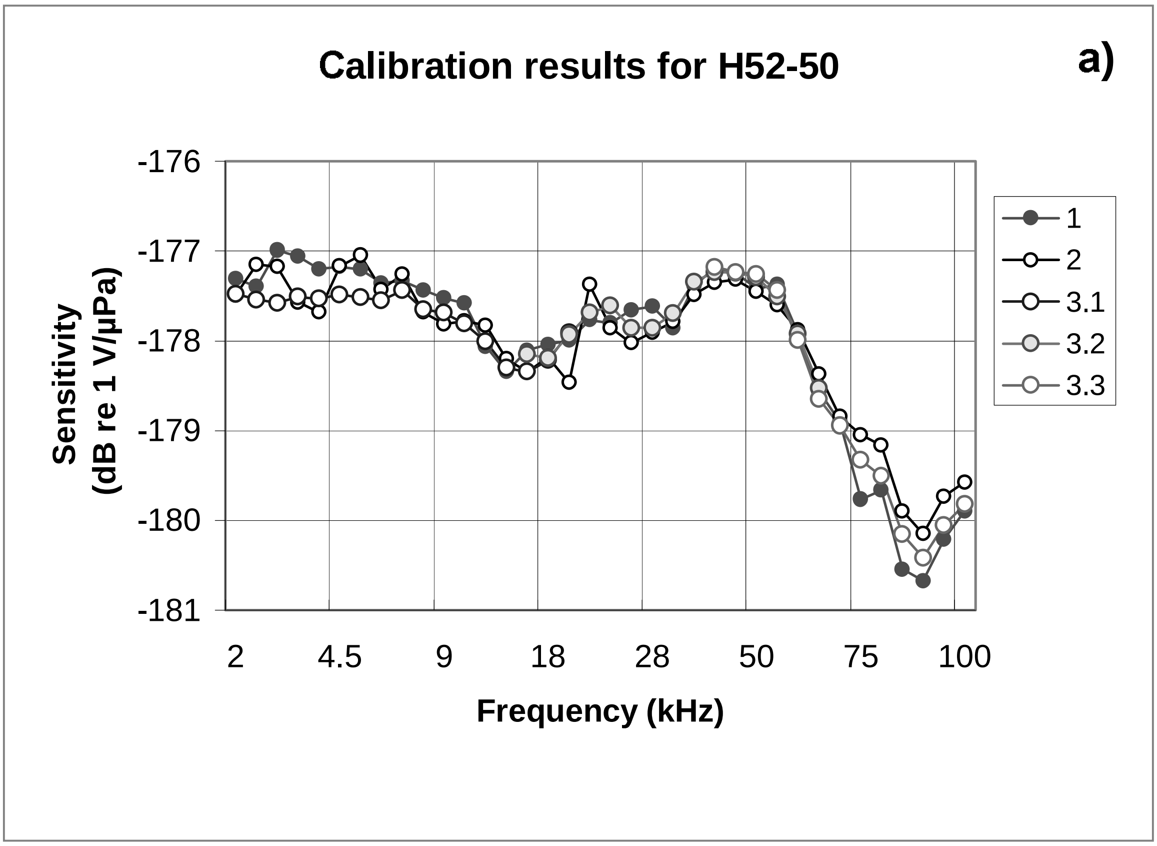
Calibration results for H52-50
a)
Sensitivity
(dB re 1 V/µPa)
-176
-177
-178
-179
-180
-181
2
4.5
9
18
28
50
75
100
Frequency (kHz)
1
2
3.1
3.2
3.3

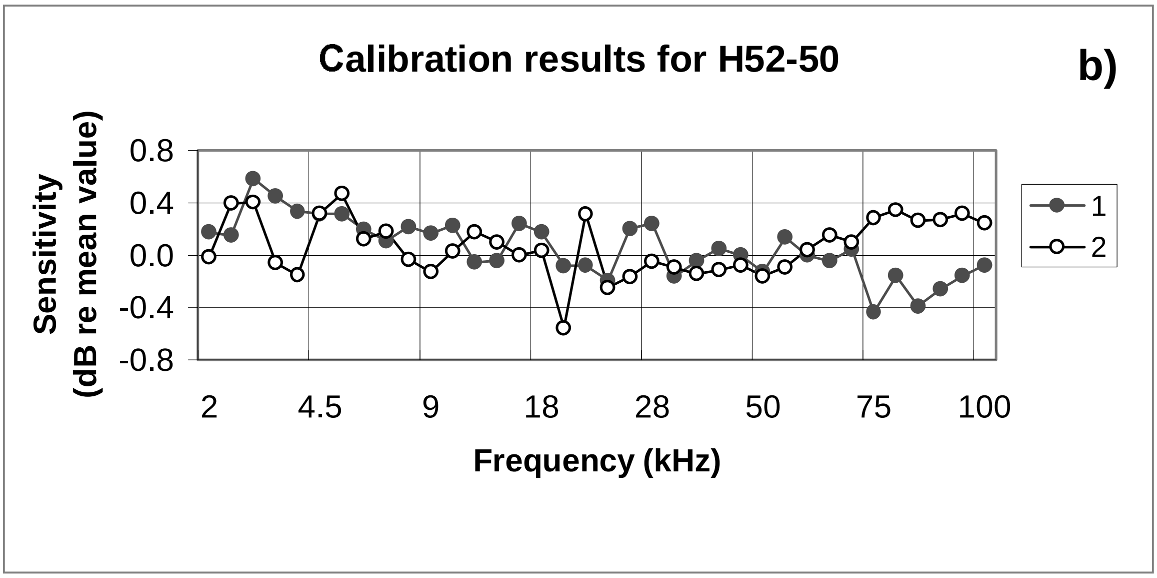
Calibration results for H52-50
b)
Sensitivity
(dB re mean value)
0.8
0.4
0.0
-0.4
-0.8
2
4.5
9
18
28
50
75
100
Frequency (kHz)
1
2

FIG. 10

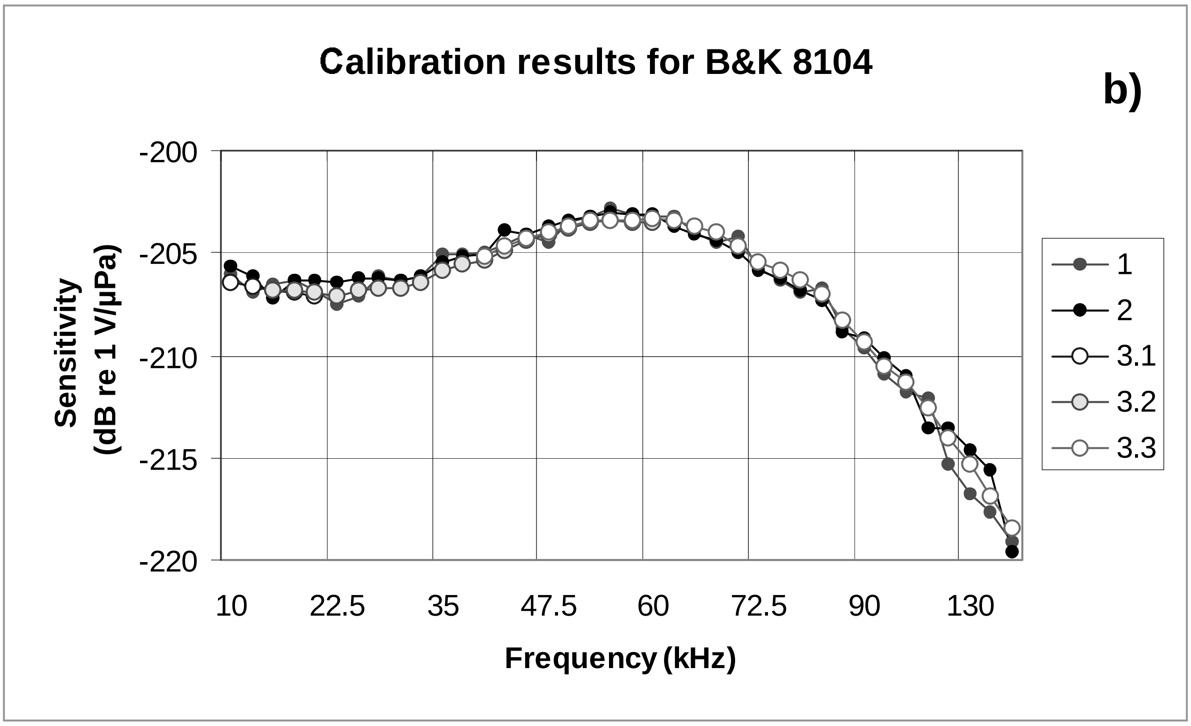
Calibration results for B&K 8104
b)
Sensitivity
(dB re 1 V/µPa)
-200
-205
-210
-215
-220
10
22.5
35
47.5
60
72.5
90
130
Frequency (kHz)
1
2
3.1
3.2
3.3

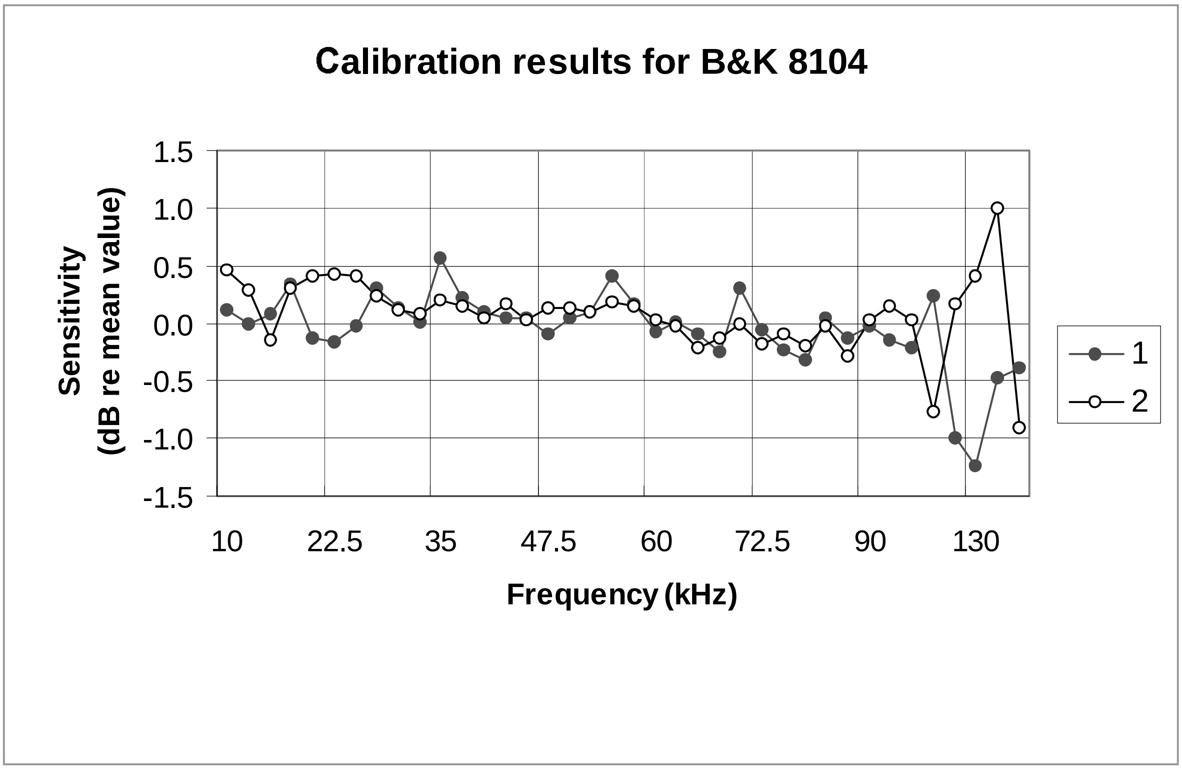
Calibration results for B&K 8104
Sensitivity
(dB re mean value)
1.5
1.0
0.5
0.0
-0.5
-1.0
-1.5
10
22.5
35
47.5
60
72.5
90
130
Frequency (kHz)
1
2

FIG. 11